HHS Public Access

Author manuscript

J Colloid Interface Sci. Author manuscript; available in PMC 2017 January 15.

Published in final edited form as:

J Colloid Interface Sci. 2016 January 15; 462: 325–333. doi:10.1016/j.jcis.2015.10.019.

Ion-ion correlation, solvent excluded volume and pH effects on physicochemical properties of spherical oxide nanoparticles

Zaven Ovanesyan, **Amal Aljzmi**, **Manal Almusaynid**, **Asrar Khan**, **Esteban Valderrama**, **Kelly Nash**, and **Marcelo Marucho***

Department of Physics and Astronomy, The University of Texas at San Antonio, San Antonio, TX 78249-5003

Abstract

One major source of complexity in the implementation of nanoparticles in aqueous electrolytes arises from the strong influence that biological environments has on their physicochemical properties. A key parameter for understanding the molecular mechanisms governing the physicochemical properties of nanoparticles is the formation of the surface charge density. In this article, we present an efficient and accurate approach that combines a recently introduced classical solvation density functional theory for spherical electrical double layers with a surface complexation model to account for ion-ion correlation and excluded volume effects on the surface titration of spherical nanoparticles. We apply the proposed computational approach to account for the charge-regulated mechanisms on the surface chemistry of spherical silica (SiO_2) nanoparticles. We analyze theeffects of the nanoparticle size, as well as pH level and electrolyte concentration of the aqueous solution on the nanoparticle's surface charge density and Zeta potential. We validate our predictions for 580 Å and 200 Å nanoparticles immersed in acid, neutral and alkaline mono-valent aqueous electrolyte solutions against experimental data. Our results on mono-valent electrolyte show that the excluded volume and ion-ioncorrelations contribute significantly to the surface charge density and Zeta potential of the nanoparticle at high electrolyte concentration and pH levels, where the solvent crowding effects and electrostatic screening have shown a profound influence on the protonation/deprotonation reactions at the liquid/solute interface. The success of this approach in describing physicochemical properties of silica nanoparticles supports its broader application to study other spherical metal oxide nanoparticles.

Abstract

*marcelo.marucho@utsa.edu (Marcelo Marucho).

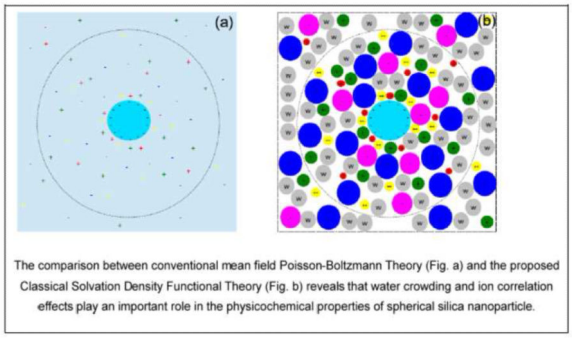

The comparison between conventional mean field Poisson-Boltzmann Theory (Fig. a) and the proposed Classical Solvation Density Functional Theory (Fig. b) reveals that water crowding and ion correlation effects play an important role in the physicochemical properties of spherical silica nanoparticle.

Keywords

Surface charge density; Zeta potential; Density functional theory; Nanoparticles; Surface chemistry

1. Introduction

Physicochemical properties of nanoparticles (NPs), such as particle size (PS), Zeta potential (ZP) and surface charge density (SCD), have significant effects on their cellular uptake[1, 2, 3], colloidal aggregation[4, 5] and stability[6, 7, 8, 9]. The biodistribution and pharmacokinetic properties of NPs in the body depend on PS and SCD. For instance, modification of the SCD provides controlled binding of NPs to the tissue and targets them to specific sites inside the cell[9], and consequently, affects the behavior of NPs in bio-logical environment[10]. In particular, PS, SCD and ZP of NPs influence the properties of nano-medicines, such as stability of dosage forms, their release rate at specific sites, NP circulation in the blood and absorption of a drug into body membranes[11].

Highly positive or negative ZP values introduce large repulsive forces, preventing particles with similar electric charge from aggregation and ensuring redispersion in aqueous electrolyte solutions[12, 13, 14]. Therefore, the NP aggregation can be controlled by changing the ZP[15], which may improve the dosage stability and increase drug release rate at specific sites. The ZP can be efficiently controlledby pH modification, which is a useful approach for measuring NP toxicity[16]. Overall, the stability of NPs depends on the medium, as well as the physical characteristics of the suspended NPs[16]. Beyond the important role of these physicochemical properties of NPs in biological environment, the relationship between ZP, SCD, and electrolyte solution surrounding the NPs is still a widely unexplored area.

Typically, when a NP is immersed in an aqueous medium, its surface reveals a charge-regulated nature due to the protonation/deprotonation reactions of the dissociable functional groups at the solid/liquid interface[17, 18]. Due to the resulting interaction between the surface charge and dissolvedions the later form the electrical double layer (EDL) around the charged NP[18, 19]. More counterions tend to accumulate, whereas co-ions tend to deplete within the EDL. The surface complexation (SC) models are used to describe this charging process, where an ensemble of mass balance equilibrium and associated constants account

for the titration of surface groups. The SC models such as the constant capacitance model, the diffuse layer model, and the triple layer model, differ in their structural representation of the solid/solution interface[20].

Several theoretical approaches have been proposed to study EDL and titration properties of NPs. One of the most used approaches is based on the Poisson-Boltzmann (PB) equation due to its high efficiency in describing electrostatic properties of biomolecules immersed in dilute mono-valent electrolyte solutions. Generally, the ion density profiles around NPs are approximated by a Boltzmann distribution, which depends on the ionic potential of mean force. The main assumption underlying the PB approach is that the ionic potential of mean force can be replaced with the mean electrostatic potential. Additionally, the discrete nature of the solvent and ion-ion correlations are completely ignored (see Figure 1a). When these ingredients are taken into account properlyand efficiently, it is possible to provide a more realistic description of the structural and thermodynamic properties of charged NPs interacting with liquids (see Figure 1b). For instance, ion-ion correlation in solutionsof charged NPs has attracted much interest due to its ability to generate net attractive forces between equallycharged NPs[21]. An equally important aspect of ion-ion correlation is its facilitation of surface titration processes[22]. Moreover, the incorporation of neutral solvent molecules in spherical electrical double layer (SEDL) models has shown to give rise to layering formation in ion and solvent density profiles and to induce charge inversion[23]. Computer simulations of atomic models with explicit waterand ions represent the most detailed method to study the influence of salt solutions on the physicochemical properties of nanoparticles. However, such explicit solvent simulations of NPs in dilute electrolytes can be computationally very expensive.

To overcome some of these limitations, we recently introduced a classical solvation density functional theory (CSDFT) for EDLs of spherical NPs that extends the capabilities of PB theory by taking into account electrostatic ion-ion correlations, size asymmetry and excluded volume effects without increasing significantly thecomputational cost[24]. We demonstrate that the presence of solvent molecules with experimentallyknown concentration and size values has a significant impact on the layering of ions, the competition between the ionic charge correlations and the solvent excluded volume effects governing the SEDL properties. For instance, the layering formation directly influences the mean electrostatic potential and ion density profiles in the diffuse region of the SEDL and has noticeable impact on the behavior of ZP and the number of ions accumulated near the nanoparticle surface. Beyond the success of the current version of this approach in describing the structural and thermodynamic properties of spherical charged NPs, it is unable to account for the effects of the pHon the SCD of the NP.

In this article, we extend the aforementioned CSDFT to account for the charge-regulated mechanisms of the NP surface on the structural and thermodynamics properties of SEDLs. We combine the CSDFT with a surface complexation model to account for ion-ion correlation and excluded volume effects on the surface titration of spherical NPs. We apply the proposed computational approach to describe the role that the ion size and solvent excluded volume play on the surface titration properties of silica NPs. We analyze the effects of the NP size, pH and salt concentration of the aqueous solution on the NP surface

charge density and Zeta potential. We describe the role that these properties play on mono-valent ion preferential selectivity by silica NPs. We analyze NaCl electrolytes at several concentrations and pH levels. In this article, we choose silica NPs as a representative model of spherical oxide NPs because of the availability of theoretical and experimental studies[18, 25, 26, 27] and its broad applications[28, 29, 30]. However, the proposedtheoretical approach can be applied to other spherical metal oxide NPs.

2. Materials and methods

2.1. Classical solvation density functional theory for spherical electrical double layer

The system considered in this approach consists of a rigid charged spherical nanoparticle surrounded byan electrolyte solution comprised of *m* ionic species as described elsewhere[24]. Here, we provide important details on the models used to study silica nanoparticles. Each ion of species *i* is represented by bulk Molar concentration $\left[\rho_i^0\right]$, a charged hard sphere of diameter d_i, and total charge $q_i = ez_i$, where *e*is the electron charge and z_i is the corresponding ionic valence (see Figure 1b). The solventmolecules are represented using the primitive model approach in which the electrostatics is considered implicitly by using the continuum dielectric environment with a dielectric constant $E = 78.5$, but the steric interaction is incorporated explicitly by considering the solvent molecules as a neutral hard sphere. The charged spherical silica nanoparticle is represented by a hard sphere of radius *R* and uniform surface charge density σ that arises from the surface titration of the nanoparticles as described below. The presence of the silica nanoparticle in the bulk electrolyte is modeled as an external potential $v_i(r)$ acting on each ion species *i*. The resulting inhomogeneous ion profiles $[\rho_i(r)]$ are calculated using a classical solvation density functional theory recently introduced by B. Medasani et. al. [24] as follows:

$$[\rho_i(r)] = \left\{ \left[\rho_i^0\right] exp\left\{-\beta q_i \psi(r,[\rho_j])\right\} + \Delta c_i^{(1)hs}(r;\{[\rho_j]\}) + \Delta c_i^{(1)res}(r;\{[\rho_j]\}) \right\}, r > R+\sigma_i/2 \quad 0, r \le R+\sigma_i/2 \quad (1)$$

where $\beta = 1/kT$, *k* is the Boltzmann constant, *T* the temperature (298.15K), $\psi(r, \{[\rho_j]\})$ represents the mean electrostatic potential, and $c^{(1)hs}(r; \{[\rho_j]\})$ and $c^{(1)res}(r; \{[\rho_j]\})$ are the hard sphere and residual electrostatic ion-ion correlation functions, respectively. The hard spherecontribution is estimated by using the White Bear version II of the Fundamental Measure Theory (WBFMT-II)[31], whereas the electrostatic ion correlation effects are taken into account by utilizing a leading functional Taylor expansion approximation in power of the ion density profiles and the Mean Spherical Approximation(MSA) for multicomponent charged hard sphere fluids[32, 33]. When Eq. (1) is coupled with the Poisson equation for an homogeneous anisotropic dielectric media ε

$$\nabla^2 \psi(r,\{[\rho_j]\}) = -\frac{1}{\epsilon}\sum_{i=1}^{m}[\rho_i(r)]z_i, \quad (2)$$

we obtain the following master equation for the electrical double layers of spherical nanoparticles:

$$\nabla^2\psi\left(r,\{[\rho_j]\}\right)=-\frac{1}{\epsilon}\sum_{i=1}^{m}z_i\left[\rho_i\right]exp\left\{-\beta q_i\psi\left(r,\{[\rho_j]\}\right)+\Delta c_i^{(1)hs}\left(r;\{[\rho_j]\}\right)+\Delta c_i^{(1)res}\left(r;\{[\rho_j]\}\right)\right\}$$
$$\epsilon\partial\left(r;\{[\rho_j]\}\right)/\partial r|_{r=s}=-\sigma,\qquad \psi\left(r;\{[\rho_j]\}\right)|_{r\to\infty}\to 0. \tag{3}$$

The expressions for $\Delta c_i^{(1)hs}\left(r;\{[\rho_j]\}\right)$ and $\Delta c_i^{(1)res}\left(r;\{[\rho_j]\}\right)$ are given in reference[24].

These additional terms $\Delta c_i^{(1)hs}\left(r;\{[\rho_j]\}\right)$ and $\Delta c_i^{(1)res}\left(r;\{[\rho_j]\}\right)$ appearing in Eq. (3) provide corrections to the continuum PB predictions, and may be responsible for capturing charge inversionionic layering formation and other important phenomena characterizing colloidal systems. Note that Eq. (3) describes how changes on the mean electrostatic potential (left-hand side) are induced due to the ionic electrostatic potential energy, excluded volume, ion-ion correlation, and nanoparticle surface charge density and size (right-hand side and boundary conditions). In particular, the solution of the mean electrostatic potential at the surface charge layer position *s* accounts for the ion-ion correlations, size asymmetry and excluded volume effects on the ZP ($\zeta\equiv\psi(r,\{[\rho_j]\})|_{r=s}$). Certainly, the position of the surface charge layer depends on the electrolyte model used to describe the EDL properties. In the simplest case, where ionic size effects are omitted[34] (e.g. using PB theory alone), the surface charge layer lies on the nanoparticle's surface $s = R$. However, the location of the SCD layer is not well defined in more realistic electrolyte models which predict multilayering formation due to ion correlation and exclude volume effects. In this article, we find that SCD layers formed at $s = R+ <\{d_i\}>$, where $<\{d_i\}>\equiv N_A\lambda_B^3\sum_i z_i^2\left[\rho_i^0\right]d_i/(2m)$, provides the SCD and the ZP predictions, which are in good agreements with the experimental data for silica nanoparticles at low and high bulk electrolyte concentrations and for different nanoparticle sizes (See validation section). In the later definition, N_A and λ_B stand for the Avogadro number and the Bjerrum length, respectively. Interestingly, the expression proposed for $<\{d_i\}>$ resembles the definition of the ionic strength and may represent an average of the ionic radius weighted by their charge density, making ion species at high concentrations and large sizes play a dominant role in the position of the SCD layer. In particular, high electrolyte concentrations tend to decrease the magnitude of the ZP, whereas low electrolyte concentrations make the dependence of the ZP on the ionic size rather weak. Our definition of the SCD layer position also depends on the Bjerrum length $\lambda_B\equiv e^2/(4\pi\varepsilon_o\varepsilon K_B T)$ for dimensional unit purpose, as well as to account for solvent dielectric constant ε and thermal energy scale K_BT effects. For example, high solvent permittivity constants generate strong electrostatic screening and, consequently, the SCD formation closer to the surface of a spherical nanoparticle. In addition, high thermal energy scales decrease the magnitude of electrostatic interactions, which attenuates the mean electrostatic potential near the nanoparticle surface. Clearly, the position $s = R+ <\{d_i\}>$ recovers the mean-field (e.g. PB) approximation position ($<\{d_i\}>= 0$) for point-like ions by setting $d_i = 0$. Moreover, the SCD layer is formed closer to the nanoparticle surface at low ionic densities for all ion sizes.

Note that the CSDFT described above for SEDLs assumes that the surface charge density of the nanoparticle is not affected by the presence of the surrounding ions, free protons and water molecules. It is also unable to account for the ionization of the active functional groups distributed on the surface of the metal oxide nanoparticle. In the next subsection, we

incorporate these elements into the CSDFT for SEDLs using an extended surface complexation model.

2.2. Surface complexation model

In order to account for the regulation on surface charge density of the spherical nanoparticle σ due to the titration[34] we consider two protonation reactions of single M-coordinated sites with equilibrium constants K_A and K_B as follows:

$$MOH \leftrightarrow MO^- + H^+, \qquad MOH + H^+ \leftrightarrow MOH_2^+ \quad (4)$$

The equilibrium constants are defined by

$$K_A = \frac{N_{MO^-}[H^+]_s}{N_{MOH}}, \qquad K_B = \frac{N_{MOH_2^+}}{N_{MOH}[H^+]_s} \quad (5)$$

In the above, $N_{M\,OH}$, $N^{M\,O^-}$, and $N_{M\,OH^+}$ are the surface site densities of *M OH*, *M* O^- and *M* OH^+, respectively, and $[H^+]_s$ is the concentration of H^+ ions at the solid/liquid interface *s* which follows the ion density distribution (1) predicted by the CSDFT for SEDLs

$$\left[H^+\right]_s \equiv [\rho H(r)]_{r=s} = \left[\rho_H^0\right] exp\left\{-\beta\zeta + c_H^{hs} + c_H^{res}\right\}, \quad (6)$$

where ζ is the ZP, and $c_H^{hs} \equiv \Delta c_H^{(1)hs}$ and $c_H^{res} \equiv \Delta c_H^{(1)res}$ are the excluded volume and ion-ion correlation contributions to the concentration of H^+ ions at the surface, respectively. $[\rho^0]$ represents the bulk concentration of H^+ ions, which is related to the *pH* value of the bulk liquid at infinity dilution by the expression $pH = -Log\left(\left[\rho_H^0\right]\right)$. Clearly, the proposed Eqs. (6) and (5) account not only for the mean-field contribution, e.g. the ZP, but also for the ion-ion correlation and excluded volume effects on the surface titration of spherical nanoparticles. The total number site density of functional groups on the solid/liquid interface is $N_{total} = N_{MO-} + N_{MOH} + N_{MOH_2^+}$ and the SCD is $\sigma = -F\left(N_{MO-} - N_{MOH_2^+}\right)$. Writing the densities sites in terms of the equilibrium constants (6) we obtain:

$$\sigma = \sigma\left(pH, K_A, K_B, N_{total}, \alpha, c_H^{hs}, c_H^{res}, \beta\right) = -FN_{total}\frac{K_A - K_B\left[\left[\rho_H^0\right] exp\left\{-\beta\zeta + c_H^{hs} + c_H^{res}\right\}\right]^2}{K_A + \left[\rho_H^0\right] exp\left\{-\beta\zeta + c_H^{hs} + c_H^{res}\right\} + K_B\left[\left[\rho_H^0\right] exp\left\{-\beta\zeta + c_H^{hs} + c_H^{res}\right\}\right]^2}$$

As a result, Eq. (7) describes the charging mechanisms of the surface of the spherical nanoparticle, which depend on the temperature, the ZP, the ion correlation and excluded volume at the solid/liquid interface, the pH of the bulk liquid, and the total site density of the functional groups, among other physicochemical properties of the nanoparticle. Note that Eq. (7) becomes the mean-field approximation for the SCD when the new two contributions c_H^{hs} and c_H^{res} and the ionic diameters are set equal tozero[18].

In the next subsection we describe the electrolytes used in these studies to model the effects of the SEDL on the SCD and ZP.

2.3. Electrolyte solutions and surface titration characterization

In this work, we consider silica oxide nanoparticles immersed in multiple electrolyte solutions, where the surface titration of the nanoparticle is represented by a total density number of active functional group $N_{total} = 2 * 10^{-6} mol/m^2$ and equilibrium constants $pK_A = -log(K_A) = 6.8$ (protonation) and $pK_B = -log(K_B) = 1.7$ (deprotonation)[34]. We model a single salt comprised of mono-valent ions (NaCl) at various concentrations and pH levels. The *pH* of the solution is adjusted by adding NaOH and HCl solutions to the electrolyte. The resulting electrolyte solutions contain five (Na^+, Cl^-, H^+, OH^-, H_2O) ion species. The free proton and hydroxyl ion bulk concentrations are given by the well-known expressions $\left[\rho_H^0\right] = 10^{-pH}, \quad and \quad \left[\rho_{OH}^0\right] = 10^{-(14-pH)}$ respectively, and the bulk concentrations of the electrolyte are chosen to satisfy the bulk electroneutrality condition.

2.4. Computational scheme

The coupled Eqs. (7) and (3) are solved numerically using conventional Picard iterative-like solvers. We use the pH, ions and solvent molecules bulk concentrations and sizes, temperature, nanoparticle size, equilibrium constants and total site density number as the input parameters of the theory. First, we assign a null value for the initial guess of the surface charge density into Eq. (3) to numerically calculate the ion density profiles, ion correlation, excluded volume and mean electrostatic potential using the computational scheme described in reference[24]. Second, we evaluate these expressions at the solid/liquid interface to obtain the numerical values for ζ, $c_H^{hs}, \quad \text{and} \quad c_H^{res}$. Finally, we replace these values into Eq. (7) to obtain the new surface charge density estimation for the next iteration. The iteration will stop when the relative error between the old and the new surface charge density estimations is smaller than the required tolerance (1% in our case). To improve the stability and convergence of the numerical solution we implement the mixing parameter approach where the new estimation of the surface charge density is a linear combination of the current and previous estimations. The computing time obtained with one CPU processor depends on the mixing parameter value, and the electrolyte and nanoparticle models. For example, the PB results for a nanoparticle with 580 Å radius immersed in NaCl electrolyte at 0.001 M concentration and pH = 5.0 are produced in 9 seconds, whereas the CSDFT approach generates these results in 307 seconds.

3. Results and discussion

In this section, we study the properties of surface complexation using PB and CSDFT. For that purpose, we first validate our predictions against the available experimental data. Then, we study different scenarios in which the silica nanoparticle size and background salt concentration and pH level affect the surface charge density and Zeta potential of the silica nanoparticle.

3.1. Validation of the proposed computational model against available experimental data

The comparison of the theoretical predictions against experimental data is a useful strategy for verifying the accuracy of the physical approximations and model parameters used to describe the experimental observations. We calculate the surface charge density for a 580 Å radius nanoparticle immersed in NaCl at several electrolyte concentrations and pH solutions. Our CSDFT results (dashed lines) are presented in Figure 2 and compared with experimental data (symbols)[34] and PB predictions (solid lines). Notice that PB and CSDFT use different location for the SCD position. Also, ion-ion correlation and excluded volume contributions are not included in the PB but are considered in the CSDFT model. Beyond these differences between the PB and the CSDFT approaches, they predict similar SCD values for mono-valent salts at low electrolyte concentrations (see Figure 2). Additionally, these predictions are in a very good agreement with experimental results. These comparisons suggest that aforementioned differences between the two approaches seem to be irrelevant under these experimental conditions. This is attributed to the insignificant influence of ion-ion correlation and excluded volume effects on the SCD and the ZP at low electrolyte concentrations. Under these experimental conditions, the contribution $< \{d_i\} >$ to the position of the SCD layer s is very small, generating a very similar location for both approaches, e.g. $s_{SCDFT} \simeq s_{PB} = R$. Overall, the CSDFT must recover PB predictions if the diameter of ions are set equal to zero and the ion-ion correlation and excluded volume contributions are switched off in our model.

We further validate our approach in predicting the ZP for a 200 Å radius silica nanoparticle immersed in 0.8 Molar NaCl concentration at several pH solutions. Our CSDFT results (green squares) are presented in Figure 3 and compared with experimental data (black circles) and PB predictions (red diamonds). A detailed description of the materials and methods used in the experiments is provided in the appendix. Clearly, our predictions are in good agreement with the experimental data. On contrary, the PB results deviate significantly from our predictions and experimental data, mainly at high pH levels, due to the high value of the ionic strength which increases the magnitude of the omitted ion correlation and exclude volume contributions to the mean electrostatic potential decay rate near the nanoparticle surface. Ion correlation and exclude volume interactions also increase the position $s_{PB} = R$ of the SCD layer formation by the distance $< \{d_i\} >= 4.5$ Å which is neglected in PB. The detailed description of the ionic strength effects on the SCD and the ZP is provided below.

3.2. Role of ion correlation, excluded volume and pH on Zeta potential and surface charge density of silica nanoparticles

In this subsection, we present a comprehensive analysis to advance the understanding of the role of ion-ion correlation, excluded volume and pH on the ZP and the SCD of silica nanoparticles. First, we study these two physicochemical properties for different nanoparticle sizes immersed in fixed background of mono-valent electrolyte concentrations as a function of pH (see Figure 4). This study provides useful information on the nanoparticle size and pH effects on the ZP and the SCD under different environmental conditions. In the second analysis, we fix the nanoparticle size but change the electrolyte concentration of mono-valent salts (see Figures 6 and 7). This study provides insight on the

effects of multiple background electrolyte environments and pH on the ZP and the SCD for fixed nanoparticle sizes. Overall, in all these studies we compare the PB versus the CSDFT predictions to determine the role that ion-ion correlation and excluded volume play on the ZP and the SCD as a function of pH, nanoparticle size and ionic strength.

3.2.1. Analysis for several nanoparticle sizes and fixed background electrolyte

The results of the first study are presented in Figure 4 a), which represents the surface charge densities of silica nanoparticles with five radii (5 Å, 15 Å, 40 Å, 200 Å and 580 Å), pH levels between 4 and 8, and 0.4 NaCl concentration. Figure 4 a) shows that both PB (solid lines) and CSDFT (dashed lines) results predict an increase of the SCD with decreased nanoparticles sizes. These approaches also predict that the magnitude of the surface charge density increases as pH raises. This behavior is in agreement with the experimental data shown in Figure 2, and also agrees qualitatively with previous work[18]. The largest negative SCD is predicted for the smallest nanoparticle size, whereas the smallest negative SCD is predicted for the largest nanoparticle size. According to Eq. (5), the bulk concentration of H^+ ions decreases with increased pH levels, which leads to an increase in the number of functional groups deprotonated on the surface. Consequently, the SCD becomes more negative. The comparison between PB and CSDFTpredictions presented in Figure 4 a) reveals the importance of the excluded volume and ion-ion correlation effects in the charging mechanisms of the SCD. For small nanoparticles, these additional contributions increase themagnitude of the surface charge predicted by PB, whereas for large nanoparticle sizes, there is smaller increase in magnitude of the SCD. This comparison also shows larger excluded volume and ion-ion correlation contributions at increased pH levels. Another important difference between PB and CSDFT predictions is given for large silica nanoparticles. In the limit of infinitely large spherical nanoparticles, PB and CSDFT results are expectedto reproduce those predicted for flat charged surfaces. Our results show that the same critical nanoparticle size of 200 Å is predicted by both models, after which the nanoparticle curvature effects become negligible (see purple and black lines in Figure 4a and b). At 0.4M electrolyte concentration there is a remarkable difference between PB and CSDFT predictions due to the ion-ion correlation and excluded volume contributions accounted by CSDFT. The most significant differences between PB and CSDFT predictions are observed for high pH levels, large nanoparticle sizes, and high ionic strength. This is mainly due to the solvent crowding effects in which many solvent molecules are pushing ions toward the surface of the nanoparticle. As a consequence, larger nanoparticlesaccumulate higher number of ions around the nanoparticle. This in turn generates higher electrostatic screeningwhich reduces the net charge of the nanoparticle surface[24].

To understand the relationship between the SCD and the ZP behavior for different silica nanoparticle sizes, we present in Figure 4 b) the ZP as a function of the pH for the same nanoparticle sizes and fixed electrolyte concentrations described in Figure 4 a). The variation of ZP with pH may be understood in terms of the analysis previously done for the SCD, the explicit but not trivial relationship between ZP and SCD given by the complexation model (7) and the Debye-Hückel theory. The later approach, when applied to spherical charged particles immersed in electrolytes at neutral pH, provides the following

simple approximate expression $\zeta = \psi(r, \{[\rho_j]\})|_{r=s} \simeq Q exp(-sK(\{[\rho_j]\}))/[\epsilon s(1+KR)]$ to calculate the ZP generated by a nanoparticle of size R and (fixed) homogeneous surface charge density σ, total nanoparticle charge $Q = 4\pi\sigma R^2$, Debyescreening length $K \sim \sqrt{I}$, ionic strength $I = \sum q_i^2 \left[\rho_i^0\right]$, and bulk dielectric constant ε. This expression (valid for dilute mono-valent electrolytes) predicts that the magnitude of the ZP depends linearly on the total nanoparticle charge, which accounts not only for the SCD but also the nanoparticle surface area contributions. Clearly, the larger the nanoparticle charge, the larger the magnitude of the ZP. On the other hand, an increase in the ionic strength yields an exponential decrease of the effective nanoparticle charge due to a large electrostatic screening. As a result, the magnitude of the ZP decreases. Therefore, for a given (fixed) nanoparticle size, anincrease of the pH level increases the SCD (see Figure 4 a)), and consequently, increases the magnitude of the corresponding ZP (see Figure 4 b)). On the other hand, for a given pH level, larger nanoparticles induce smaller SCD (see Figure 4 a)) along with an increase of the total nanoparticle charge (see Figure 5). Consequently, the magnitude of the ZP decreases (see Figure 4 b)). For instance, Figure 5 shows that the total charge $Q = 4\pi\sigma s^2$ for a silica nanoparticle immersed in 0.4 M NaCl concentration and pH = 8 is $Q_{5A} \simeq -3.14e$ for PB and $Q_{5A} \simeq -7.51e$ for CSDFT, whereas the one corresponding to 580 Å and same pH is $Q_{580A} \simeq -33,444e$ and $Q_{580A} \simeq -44,542e$, respectively. Therefore, smaller nanoparticles generate larger SCDs but smaller ZPmagnitudes. This behavior is also observed in Figure 4 once the ion-ion correlation and excluded volume effectsare taken into account in the calculation of the SCD and ZP. In this case, the interplay between ZP and SCD is described by our proposed complexation model (Eq. 7) in a non-trivial manner. The comparison between PB and CSDFT predictions on the ZP show that ion-ion correlationand excluded volume contributions become more important for small nanoparticles and high pH levels. For instance, at pH = 8 and 0.4 NaCl salt concentration, PB predicts ZP around −75 mV and −55 mV for silicananoparticles of 580 Å and 5 Å sizes, respectively. Whereas, the consideration of the solvent excluded volume and ion-ion correlation effects alter these ZP values to −44 mV and −25 mV, respectively. As a result, these two contributions decrease the PB predictions on the ZP by 40% to 55% approximately. Figure 4 b) shows that 0.4M salt concentration produces strong electrostatic screening, reducing the magnitude of the ZP. At high pH levels, the surface charge becomes more negatively charged. This in turn increasesthe ZP, which is given by the value of the mean electrostatic potential at the surface. More details on the effects of ionic strength on the SCD and the ZP are given below.

3.2.2. Analysis for several background electrolytes and fixed nanoparticle sizes

Figure 6 represents the surface charge density of silica nanoparticles with four NaCl salt concentrations (0.01 M, 0.1 M, 0.4 M and 0.8 M), pH range between 4 and 10 and three nanoparticles sizes, e.g. 5 Å radius (Figure 6a), 15 Å radius (Figure 6b) and 40 Å radius (Figure 6c).

In this analysis, the range of pH values is increased up to 10 in order to capture the charging saturation limit on SCD and ZP. Both PB and CSDFT predict an increase of the surface

charge density with an increase in the bulk salt concentration. These results are in agreement with the analysis based on the Debye-Hückel theory and previous work[33], where an increase in electrolyte concentration was found to increase the local concentration of Na^+ ions and decrease the local concentration of H^+ ions. Interestingly, the saturation limit for small nanoparticles (5 Å) is reached in the range of pH between 9.5 and 10 for all the electrolyte concentrations, whereas for 15 Å and 40 Å nanoparticle sizes the saturation limit dependson the electrolyte concentration. The smaller the electrolyte concentration, the higher the pH at which the saturation limit is reached. There is a critical pH value before which the SCD predictions do not depend on the electrolyte concentration and the nanoparticle size. Our results show larger critical pH values for smaller nanopar-ticles. Overall, Figure 6 reveals that the effects of excluded volume and ion-ion correlation depend on the nanoparticle size and electrolyte concentration. For 5 Å, 15 Å and 40 Å nanoparticle sizes, Figures 6 a), b) and c) show higher negative surface charge densities predicted by CSDFT compared to PB. In particular, the higher the salt concentration the higher the difference between PB and CSDFT predictions. This is mainly due to the solvent excluded volume effects which become larger at high salt concentration, where the ions are pushed toward the nanoparticle surface increasing the accumulation of Na^+ ions at the negatively charged particle surface and consequently increasing the exclusion of H^+ ions[18].

In order to understand the relationship between the SCD and the ZP behavior for different electrolyte concentrations, we present in Figure 7 the ZP as a function of pH for the same NaCl concentrations and fixed particles sizes described in Figure 6. We observe the opposite behavior in the predictions for Zeta potential compared to surface charge density. For fixed nanoparticle sizes, both PB and CSDFT models predict ZP decreasing with increased NaCl concentration. However, CSDFT predicts lower negative ZP in all the cases analyzed in this comparison. The deviation between PB and CSDFT predictions is more pronounced for high electrolyte concentrations (black lines) because the thickness ofthe EDL shorten, and consequently the ion correlation and solvent excluded volume effects compete strongly withthe mean electrostatic potential contributions[24]. On the other hand, the comparison between Figures 7 a), b) and c) show that increased nanoparticle sizes and ionic strength widen the gap between PB and CSDFT predictions with increasing pH.

4. Conclusion

In this article we extend the capabilities of recently introduced classical solvation density function theory (CSDFT) to account for the charge-regulated mechanisms of the nanoparticle surface on the structural andthermodynamics properties of spherical charged nanoparticles. We combine the CSDFT with a surface complexation model to account for ion correlation and excluded volume effects on the surface titration of spherical nanoparticles. We apply the proposed computational approach to describe the role that solvent excluded volume and ion correlations play on the surface titration properties of silica nanoparticles. We analyze the effects of the nanoparticle size, pH and salt concentration of the aqueous solution on the nanoparticle's surface charge and Zeta potential. We validate our predictions against experimental data. Our results show that the mean electrostatic potential dominates the surface titration of silica nanoparticles at low electrolyte concentrations. However, excluded volume and ion correlations contribute significantly to

the surface charge density and Zeta potential of the nanoparticle at high electrolyte concentration and pH levels, where the solvent crowding effects and electrostatic screening have a profound influence on the protonation/deprotonation reactions at the liquid/solute interface. Under such conditions, our proposed approach predicts higher negative surface charge densities for smaller nanoparticle sizes and smaller negative surface charge density for larger nanoparticle sizes when compared with those predicted by mean-field (PB) approximations. This is mainly due to the solvent crowding effects where many solvent molecules are pushing ions toward the surface of the nanoparticle. As a consequence, for larger nanoparticle sizes, there will be higher concentration of ions around the nanoparticle. This in turn generates higher electrostatic screening which reduces the net charge of the nanoparticle surface. Additionally, with an increase in electrolyte concentration there is also an increase in the concentration of counterions and decrease in concentration of H^+ ions. Thus, for a fixed nanoparticle size, more counterions are accumulated at the negatively charged particle surface with increased NaCl concentration excluding H^+ ions, which in turn increases the surface charge density. We also find that CSDFT and PB capture the effects of the nanoparticle curvature on the SCD. As a consequence, CS-DFT and PB predict same critical nanoparticle sizes, after which the nanoparticles act as flat surfaces. For low electrolyte concentration PB and CSDFT predictions of SCD are identical for these flat surfaces. However, for higher electrolyte concentration, the SCD values of flat surfaces differ between PB and CSDFT. The ZP values for mono-valent ions predicted by CSDFT reveal smaller ZP values compared to the same predictions by PB. Overall, our results reveal the limitations of mean-field approximations in capturing these effects on the surface titration of spherical charged silica nanoparticles under the influence of multiple aqueous solutions. The understanding and control of these effects are essential in designing silica nanoparticles with optimal solubility and affinity properties for specific biomedical applications. The success of this approach in describing physicochemical properties of silica nanoparticles supports its broader application to study other spherical metal oxide nanoparticles.

pH	Zeta Potential (mV)	Deviation (mV)
4	−0.260	0.110
5	−1.130	0.181
6	−4.153	0.871
7	−10.400	0.300
8	−13.300	0.781
9	−14.700	1.136
10	−13.367	0.551

Acknowledgments

This work was partially supported by the NSF-PREM Grant DMR-0934218 and NIH Grant 1SC2GM112578-01. Authors would like to thank Marcia O. Fenley for fruitful discussions and comments on the content of this paper and Jonathan Mendoza for DLS and Zeta potential measurements.

Appendix: Experimental data for 200 Å silica nanoparticles

Materials and Methods

Dispersed silica nanoparticles, 20 nm in diameter, was purchased from nanoComposix (San Diego, USA) with concentration of 10 mg/ml. NaCl, HCl and NaOH were purchased from Sigma Aldrich (St. Louis, USA). The size and Zeta potential of the nanospheres was measured using a Zetasizer ZS (Malvern Instruments Ltd.). The silica suspensions used for measurements were typically 0.12% weight of particles in water. The working volume was 1 ml for each measurement. Measurements were recorded in triplicate for both size and Zeta potential measurements.

Results

The size of the silica nanoparticles measured by the dynamic light scattering (DLS) in deionized water at 25°C. was found to be 20nm ± 2nm. This measurement is in agreement with the standard deviation reported by the manufacturer. The Zeta potentials of the silica nanoparticles were studied for a range of pH values for 0.8M NaCl electrolyte solution at 25°C.

At the lowest pH values the measured Zeta potential values are neutral to only slightly negative in value up to pH 5. Approaching pH 6 the value increases in negativity and eventually reaching an average ZP value around −13.78 mV.

References

[1]. Patil S, Sandberg A, Heckert E, Self W, Seal S. Biomaterials. 2007; 28:4600–4607. [PubMed: 17675227]

[2]. Limbach LK, Li Y, Grass RN, Brunner TJ, Hintermann MA, Muller M, Gunther D, Stark WJ. Environ. Sci. Technol. 2005; 39:9370–9376. [PubMed: 16382966]

[3]. Win KY, Feng S. Biomaterials. 2005; 26:2713–2722. [PubMed: 15585275]

[4]. Kobayashi M, Juillerat F, Galletto P, Bowen P, Borkovec M. Langmuir. 2005; 21:5761–5769. [PubMed: 15952820]

[5]. Berg JM, Romoser A, Banerjee N, Zebda R, Sayes CM. Nanotoxicology. 2009; 3:276–283.

[6]. Degen A, Kosec M. J. Eur. Ceram. Soc. 2000; 20:667–673.

[7]. Wu L, Zhang J, Watanabe W. Adv. Drug Deliv. Rev. 2011; 63:456–469. [PubMed: 21315781]

[8]. Zhang Y, Chen Y, Westerhoff P, Hristovski K, Crittenden JC. Water Res. 2008; 42:2204–2212. [PubMed: 18164742]

[9]. Honary S, Zahir F. Trop. J. Pharm. Res. 2013; 12:255–264.

[10]. Khan MK, Nigavekar SS, Minc LD, Kariapper MS, Nair BM, Lesniak WG, Balogh LP. Technol. Cancer Res. Treat. 2005; 4:603–613. [PubMed: 16292880]

[11]. Arnida MM, Janát-Amsbury A, Ray CM, Peterson H. Ghandehari, Pharm. Bio-pharm. 2011; 77:417–423.

[12]. Honary S, Zahir F. Trop. J. Pharm. Res. 2013; 12:265–273.

[13]. Patila S, Sandberg A, Heckert E, Self W, Sea S. Biomaterials. 2007; 28:4600–4607. [PubMed: 17675227]

[14]. Puttipipatkhachorn S, Nunthanid J, Yamamotoc K, Peck GE. J. Control. Release. 2001; 75:143–153. [PubMed: 11451504]

[15]. Barratt GM. Pharm. Sci. Technol. Today. 2000; 3:163–171. [PubMed: 10785658]

[16]. Berg JM, Romoser A, Banerjee N, Zebda R, Sayes CM. Nanotoxicology. 2009; 3:276–283.

[17]. Hunter, RJ. Zeta Potential in Colloid Science: Principles and Applications. Academic Press; London: 1981.

[18]. Barisik M, Atalay S, Beskok A, Qian SJ. J. Phys. Chem. C. 2014; 118:1836–1842.

[19]. Masliyah, JH.; Bhattacharjee, S. Electrokinetic and Colloid Transport Phenomena. John Wiley and Sons; Hoboken: 2006.

[20]. Goldberg, S. Chemical equilibrium and reaction models. In: Loeppert, RH., et al., editors. Soil Science Society of America Spec. Publ. 42. Soil Science Society of America; Madison: 1995.

[21]. Labbez C, Jönsson B, Skarba M, Borkovec M. Langmuir. 2009; 25:7209–7213. [PubMed: 19514750]

[22]. Jönsson B, Nonat A, Labbez C, Cabane B, Wennerström H. Langmuir. 2005; 21:9211–9221. [PubMed: 16171354]

[23]. Israelachvili J, Wennerström H. Nature. 1996; 379:219–225. [PubMed: 8538786]

[24]. Medasani B, Ovanesyan Z, Thomas DG, Sushko ML, Marucho M. J. Chem. Phys. 2014; 140:204510. [PubMed: 24880304]

[25]. Sonnefeld J, Löbbus M, Vogelsberger W. Colloids Surf., A. 2001; 195:215–225.

[26]. Huang X, Teng X, Chen D, Tang F, He J. Biomaterials. 2010; 31:438–448. [PubMed: 19800115]

[27]. Barr SA, Panagiotopoulos AZ. Langmuir. 2011; 27:8761–8766. [PubMed: 21644585]

[28]. Tan W, Wang K, He X, Zhao XJ, Drake T, Wang L, Bagwe RP. Med. Res. Rev. 2004; 24:621–638. [PubMed: 15224383]

[29]. Roy I, Ohulchanskyy TY, Bharali DJ, Pudavar HE, Mistretta RA, Kaur N, Prasad PN. Proc. Natl. Acad. Sci. 2005; 102:279–284. [PubMed: 15630089]

[30]. Barik TK, Sahu B, Swain V. Parasitol. Res. 2008; 103:253–258. [PubMed: 18438740]

[31]. Hansen-Goos H, Roth R. J. Chem. Phys. 2006; 124:154506. [PubMed: 16674241]

[32]. Blum L. Mol. Phys. 1975; 30:1529.

[33]. Hiroike K. Mol. Phys. 1977; 33:1195.

[34]. Atalay S, Ma Y, Qian S. J. Colloid Interface Sci. 2014; 425:128–130. [PubMed: 24776673]

[35]. Ovanesyan Z, Medasani B, Fenley MO, Guerrero-García GI, de la Cruz MO, Marucho M. J. Chem. Phys. 2014; 141:>225103. [PubMed: 25494770]

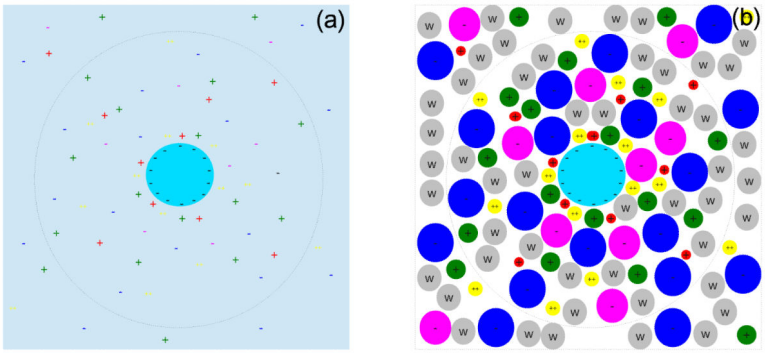

Figure 1.

The PB model a) green, red and yellow positive point charges correspond to Na^{+}, Mg^{+2} and H^{+} ions, whereas blue and magenta negative point charges represent Cl^{-} and OH^{-} ions. Silica nanoparticle is modeled as a sphere with negatively charged surface. Water is modeled implicitly as a continuum dielectric medium. The CSDFT model b) whereions are modeled as charged spheres in order to include the excluded volume effects. Sphere colors correspond to the same ions as described in the PB model. The electrostatics of the solvent is treated implicitly by using the continuum dielectric model described above, but the steric interaction is introduced explicitly by considering the solvent molecules as a neutral hard sphere. Crystalline sizes are used for ions and solvent in the CSDFT model[24].

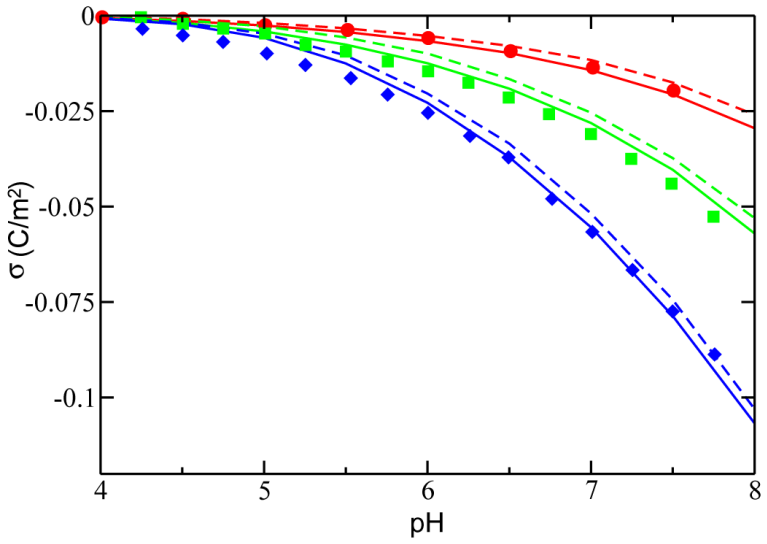

Figure 2.

Comparison of PB and CSDFT predictions of surface charge density σ for 580 Å radius silica nanoparticle immersed in different concentrations with experimental data. Red, green and blue lines represent 0.001 M, 0.01 M and 0.1 M NaCl concentrations, respectively. Solid lines represent PB predictions, whereas dashed lines correspond to CSDFT. Symbols represent experimental data[34].

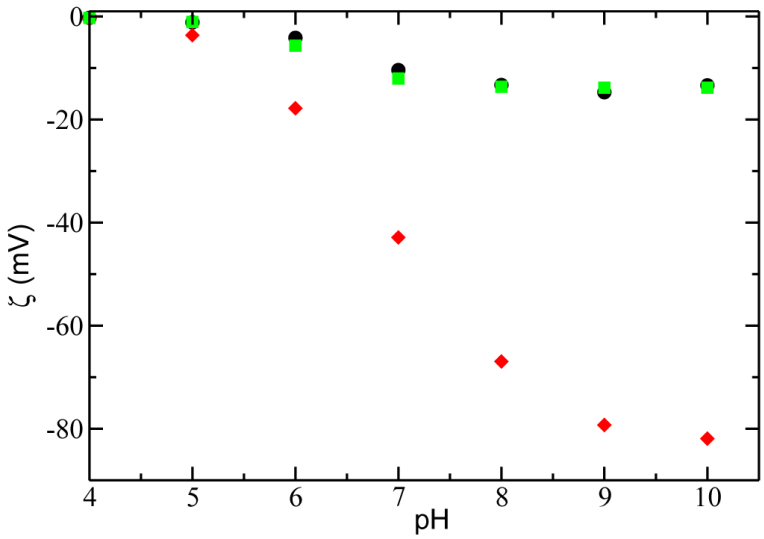

Figure 3.

Comparison of PB and CSDFT predictions of Zeta potential for 200 Å radius silica nanoparticle immersed in 0.8 M NaCl concentration with experimental data. Red diamonds, green squares and black circles represent PB, CSDFT and experimental results, respectively. The experimental error bar is not displayed in the figure because it is smaller than the circle sizes. More details on the experimental data are provided in appendix. The following surface charge layer locations s_{PB} = 200 Å and s_{CSDFT} = 204.5 Å were used for PB and CSDFT predictions, respectively.

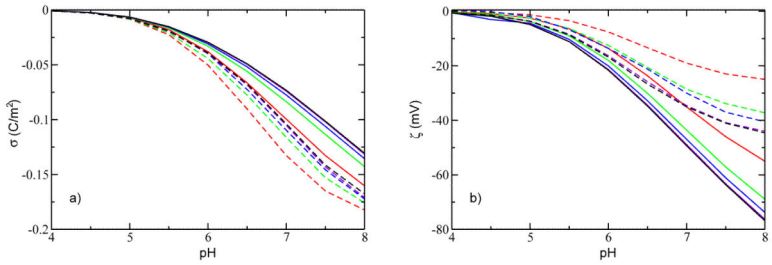

Figure 4.

Surface charge density σ (Fig. a) and Zeta potential ζ (Fig. b) of nanoparticles with different sizes in 0.4 M NaCl concentration. Red, green, blue, purple and black colors represent 5 Å, 15 Å, 40 Å, 200 Å and 580 Å nanoparticle radii, respectively. Solid lines represent PB predictions, whereas dashed line correspond to CSDFT predictions. The surface charge layer location is defined at the nanoparticle surface in PB for all ionic densities and sizes whereas in CSDFT thelayer is defined at a separation distance from the nanoparticle surface $< \{d_i\} >= 0.25$Å and $< \{d_i\} >= 2.25$ Å for 0.01M and 0.4M electrolyte concentrations, respectively.

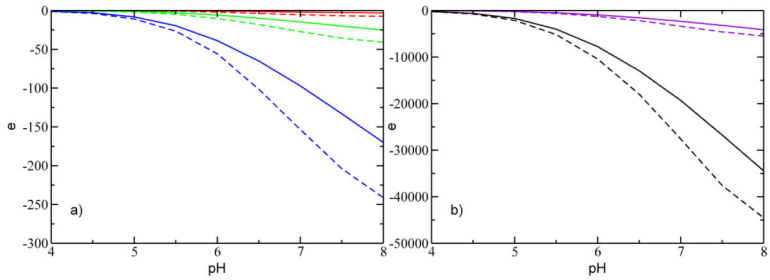

Figure 5.

Total Charge *Q* in number of electrons *e* as a function of pH. Plot a) and b) correspond for small (5 Å, 15 Å and 40 Å) and large (200 Å and 580 Å) nanoparticle sizes, respectively. Solid and dashed lines correspond to PB and CSDFT predictions, respectively.

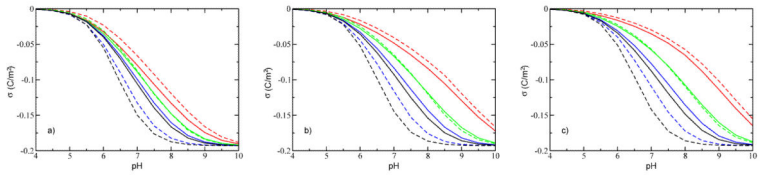

Figure 6.

Surface charge density σ as a function of pH for nanoparticles with different sizes a) 5 Å, b) 15 Å and c) 40 Å, respectively, immersed in 0.01 M (red), 0.1 M (green), 0.4 M (blue) and 0.8 M (black) NaCl electrolytes. Solid and dashed lines correspond to PB and CSDFT predictions,respectively.

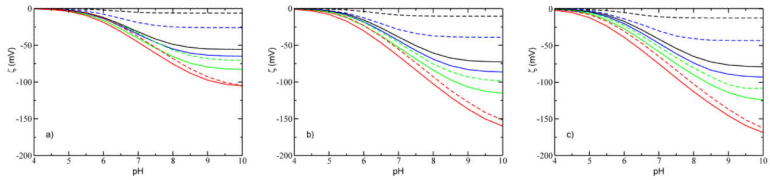

Figure 7.
Zeta potential ζ as a function of pH for the same configuration given in Figure 6.